Influence of alignment layers on crystal growth of polymer-stabilized blue phase liquid crystals

Po-Ju Chen, Michael Chen, Shih-Ya Ni, Hung-Shan Chen, and Yi-Hsin Lin*

Department of Photonics, National Chiao Tung University, Hsinchu 30010, Taiwan
*yilin@mail.nctu.edu.tw
http://web.it.nctu.edu.tw/~yilin/en/index.html

Abstract: The feature that devices based on blue phase liquid crystals (BPLCs) is free of alignment layers. However, the alignment layers could affect the morphologies of BPLC-devices as well as the electro-optical properties. In this paper, we investigate the influence of alignment layers to crystal growth of polymer-stabilized blue phase liquid crystals (PS-BPLCs). Without alignment layer, PS-BPLCs experiences both homogeneous nucleation and heterogeneous nucleation, and the morphology appears in random crystal orientations. On the contrary, when the surfaces coated with alignment layers, a heterogeneous nucleation dominates during the crystal growth process. We further proposed a possible mechanism for crystal growth under different surface condition. This study provides an alternative method to control crystal growth of PS-BPLCs, which is for facilitating many PS-BPLCs based photonic devices.

OCIS codes: (230.3720) Liquid-crystal devices; (160.3710) Liquid crystals.

References and links

1. D. C. Wright and N. D. Mermin, "Crystalline liquids: the blue phases," Rev. Mod. Phys. **61**(2), 385–432 (1989).
2. P. P. Crooker, "The blue phases. A review of experiments," Liq. Cryst. **5**(3), 751–775 (1989).
3. E. Demikhov, H. Stegemeyer, and V. Tsukruk, "Pretransitional phenomena and pinning in liquid-crystalline blue phases," Phys. Rev. A **46**(8), 4879–4887 (1992).
4. A. Hauser, M. Thieme, A. Saupe, G. Heppke, and D. Kruerke, "Surface-imaging of frozen blue phases in a discotic liquid crystal with atomic force microscopy," J. Mater. Chem. **7**(11), 2223–2229 (1997).
5. H. J. Coles and M. N. Pivnenko, "Liquid crystal 'blue phases' with a wide temperature range," Nature **436**(7053), 997–1000 (2005).
6. M. D. A. Rahman, S. M. Said, and S. Balamurugan, "Blue phase liquid crystal: strategies for phase stabilization and device development," Sci. Technol. Adv. Mater. **16**(3), 033501 (2015).
7. H. Kikuchi, M. Yokota, Y. Hisakado, H. Yang, and T. Kajiyama, "Polymer-stabilized liquid crystal blue phases," Nat. Mater. **1**(1), 64–68 (2002).
8. Y. Chen and S. T. Wu, "Recent Advances on Polymer-Stabilized Blue Phase Liquid Crystal Materials and Devices," J. Appl. Polym. Sci. **131**(15), 40556 (2014).
9. G. Nordendorf, A. Hoischen, J. Schmidtke, D. Wilkes, and H. S. Kitzerow, "Polymer-stabilized blue phases: promising mesophases for a new generation of liquid crystal displays," Polym. Adv. Technol. **25**(11), 1195–1207 (2014).
10. W. Cao, A. Muñoz, P. Palffy-Muhoray, and B. Taheri, "Lasing in a three-dimensional photonic crystal of the liquid crystal blue phase II," Nat. Mater. **1**(2), 111–113 (2002).
11. Y. H. Lin, H. S. Chen, H. C. Lin, Y. S. Tsou, H. K. Hsu, and W. Y. Li, "Polarizer-free and fast response microlens arrays using polymer-stabilized blue phase liquid crystals," Appl. Phys. Lett. **96**(11), 113505 (2010).
12. Y. H. Chen, C. T. Wang, C. P. Yu, and T. H. Lin, "Polarization independent Fabry-Pérot filter based on polymer-stabilized blue phase liquid crystals with fast response time," Opt. Express **19**(25), 25441–25446 (2011).
13. Y. H. Lin, H. S. Chen, and T. H. Chiang, "A reflective polarizer-free electro-optical display using dye-doped polymer-stabilized blue phase liquid crystals," J. Soc. Inf. Disp. **20**(6), 333–336 (2012).
14. G. Zhu, B. Y. Wei, L. Y. Shi, X. W. Lin, W. Hu, Z. D. Huang, and Y. Q. Lu, "A fast response variable optical attenuator based on blue phase liquid crystal," Opt. Express **21**(5), 5332–5337 (2013).
15. Y. Yuan, Y. Li, C. P. Chen, S. Liu, N. Rong, W. Li, X. Li, P. Zhou, J. Lu, R. Liu, and Y. Su, "Polymer-stabilized blue-phase liquid crystal grating cured with interfered visible light," Opt. Express **23**(15), 20007–20013 (2015).
16. H. S. Chen, Y. H. Lin, C. H. Wu, M. Chen, and H. K. Hsu, "Hysteresis-free polymer-stabilized blue phase liquid crystals using thermal recycles," Opt. Mater. Express **2**(8), 1149–1155 (2012).

#258217 Received 25 Jan 2016; revised 26 Feb 2016; accepted 1 Mar 2016; published 3 Mar 2016

17. M. Chen, Y. H. Lin, H. S. Chen, and H. Y. Chen, "Electrically assisting crystal growth of blue phase liquid crystals," Opt. Mater. Express **4**(5), 953–959 (2014).
18. P. Nayek, H. Jeong, H. R. Park, S. W. Kang, S. H. Lee, H. S. Park, H. J. Lee, and H. S. Kim, "Tailoring Monograin in Blue Phase Liquid Crystal by Surface Pinning Effect," Appl. Phys. Express **5**(5), 051701 (2012).
19. M. Kimura, N. Nagumo, T. N. Oo, N. Endo, H. Kikuchi, and T. Akahane, "Single-substrate polymer-stabilized blue phase liquid crystal display," Opt. Mater. Express **3**(12), 2086–2095 (2013).
20. S. Y. Lu and L. C. Chien, "Electrically switched color with polymer-stabilized blue-phase liquid crystals," Opt. Lett. **35**(4), 562–564 (2010).
21. D. Y. Kim, P. Nayek, S. Kim, K. S. Ha, M. H. Jo, C. H. Hsu, Y. Cao, S. Z. D. Cheng, S. H. Lee, and K. U. Jeong, "Suppressed Crystallization of Rod-Disc Molecule by Surface Anchoring Confinement," Cryst. Growth Des. **13**(3), 1309–1315 (2013).
22. J. Yan, S. T. Wu, K. L. Cheng, and J. W. Shiu, "A full-color reflective display using polymer-stabilized blue phase liquid crystal," Appl. Phys. Lett. **102**(8), 081102 (2013).
23. Y. Kawata, H. Yoshida, S. Tanaka, A. Konkanok, M. Ozaki, and H. Kikuchi, "Anisotropy of the electro-optic Kerr effect in polymer-stabilized blue phases," Phys. Rev. E Stat. Nonlin. Soft Matter Phys. **91**(2), 022503 (2015).
24. Y. H. Lin, T. Y. Chu, Y. S. Tsou, K. H. Chang, and Y. P. Chiu, "An electrically switchable surface free energy on a liquid crystal and polymer composite film," Appl. Phys. Lett. **101**(23), 233502 (2012).
25. K. Takatoh, M. Hasegawa, M. Koden, N. Itoh, R. Hasegawa, and M. Sakamoto, *Alignment Technologies and Applications of Liquid Crystal Devices* (Taylor & Francis, New York, 2005).
26. D. Myers, *Surfaces, Interfaces, and Colloids: Principles and Applications* (Wiley-VCH, 1999).
27. Y. H. Lin, H. Ren, Y. H. Wu, X. Liang, and S. T. Wu, "Pinning effect on the phase separation dynamics of thin polymer-dispersed liquid crystals," Opt. Express **13**(2), 468–474 (2005).
28. J. Yan, H. C. Cheng, S. Gauza, Y. Li, M. Jiao, L. Rao, and S. T. Wu, "Extended Kerr effect of polymer-stabilized blue-phase liquid crystals," Appl. Phys. Lett. **96**(7), 071105 (2010).
29. Y. Jin, C. Yuan, W. Shin-Tson, and S. Xiaolong, "Figure of Merit of Polymer-Stabilized Blue Phase Liquid Crystals," J. Disp. Technol. **9**(1), 24–29 (2013).
30. H. C. Cheng, J. Yan, T. Ishinabe, and S. T. Wu, "Vertical field switching for blue-phase liquid crystal devices," Appl. Phys. Lett. **98**(26), 261102 (2011).

1. Introduction

Blue phase liquid crystal (BPLC), a phase usually existing between the cholesteric state and the isotropic state, has been investigated for many years. BPLCs composed of double twist cylinders could be categorized in body center cubic BPI, simple cubic BPII and amorphous BPIII according to their lattice structures [1–6]. In order to extend a temperature range of the BPLCs for practical applications, polymer networks are added to BPLCs to stabilize blue phase structure under temperature fluctuations which is also known as polymer-stabilized blue phase liquid crystals (PS-BPLCs) [7]. The PS-BPLCs with a broad temperature range greatly impact device applications [8, 9], such as three dimensional mirror-less lasers [10], microlens arrays [11], Fabry Perot filters [12], a dye-doped polarizer-free display [13], variable optical attenuators [14], and grating [15]. However, hysteresis and uniformity hinder the development of PS-BPLC-based devices. Recently, we reduced hysteresis of PS-BPLC by means of competition between a homogeneous nucleation and a heterogeneous nucleation during crystal growth of PSBP-LCs under external fields, such as a thermal field or an electric field [16, 17]. We found that heterogeneous nucleation, which means the PS-BPLCs grow at the interface between two different materials or phases, has capability of suppressing homogeneous nucleation in terms of grain growth and inhibition by turns. As a result, both of the uniformity of grains and crystal orientations are controllable and then reduce hysteresis. It is well-known that devices based on BPLCs or PS-BPLCs are free of alignment layers. Nevertheless, many literatures have presented the influence of alignment to electro-optical performance of PS-BPLCs. For examples, two research groups reported the change of electro-optical properties with alignment layers of PS-BPLC, which shows the potential to improve device performance [18, 19]. Moreover, S. Y. Lu and L. C. Chien reported an electrically switched color and observed different morphologies of PS-BPLC with different alignment layers [20]. D. Y. Kim et. al. reported a suppressed crystallization of rod-disc molecule by surface anchoring confinement [21]. J. Yan et. al. demonstrated a full-color reflected displays of PS-BPLCs by assistance of surface alignment [22]. Yuto Kawata et. al. studied Kerr effect at different crystal orientations and speculated (without experimental proof) in the conclusion

#258217 Received 25 Jan 2016; revised 26 Feb 2016; accepted 1 Mar 2016; published 3 Mar 2016

that the alignment layer could affect crystal orientations of PS-BPLCs [23]. However, how alignment layer affects crystal orientation of PS-BPLCs has not been investigated, to our knowledge. By intuition, the alignment layer should affect the nucleation process during crystal growth of PS-BPLCs. In this paper, we experimentally observe the crystal growth process in three different cells, which are assembled by substrates coated with indium tin oxide (ITO) only, ITO substrates coated with parallel alignment (PA) layers, and ITO substrates coated with vertical alignment (VA) layers, respectively and proposed possible mechanism to explain the influence of alignment layer to the crystal growth of BPLCs. First, we measured the surface free energy of different substrates before assembling into cells. Then, we observed the morphology of BPLC at different temperature under microscope and further investigate the crystal orientation with Kossel diagram. Based on the experiment results, we discuss how chemical interaction and adhesion energy affect the crystal growth and final morphology with a possible mechanism. This study not only extends the understanding of crystal growth of PS-BPLCs under different surface condition, but also can expedite the development of many PS-BPLCs based electro-optical devices.

2. Sample preparation and experiments

In experiments, we used a mixture composed of a positive nematic liquid crystal (JC1041-XX, $\Delta n = 0.142$), a chiral dopant (Merck), two kinds of UV curable monomers, EHA (2-Ethylhexyl, Fluka) and RM257 (Merck), and a photo-initiator DMPAP (Aldrich) at the ratios of 56.55wt%: 35.70wt%: 3.35wt%: 3.45wt%: 0.95wt%. The measured temperature range of blue phase of the mixture was between 20 °C and 42 °C. The mixture was heated at the isotropic phase and then filled into three cells. The three cells (we called "ITO cell", "PA cell", and "VA cell" in the following manuscript) are assembled by two glass substrates with different surface treatments. The ITO cell consists of two glass substrates coated with pure indium tin oxide (ITO) layers. The PA cell consists of two ITO glass substrates coated with parallel alignment (PA) layers on which we mechanically buffered at anti-parallel directions. The VA cell consists of two ITO glass substrates coated with vertical alignment (VA) layers on which we also mechanically buffered at anti-parallel directions. After three cells were cooled down to blue phases (~27 °C) at the rate of 0.5 °C /min, the cells were exposed to an ultraviolet (UV) light (1.5 mW/cm^2) for 60 minutes for photo-polymerization to form PS-BPLCs.

To measure the surface free energy of substrates of three cells, we measured the advancing angle and receding angle of deionized (DI) water at each surface to calculate the surface free energy of the substrates [24]. Moreover, the surface free energy of the mixture (i.e. BPLC) was evaluated through Pendant drop measuring system [24]. Figure 1(a) shows that the surface free energy for substrates of three cells. The surface free energy of ITO cell, PA cell and VA cell are ~27.9×10^{-3} J/m^2, ~28.9×10^{-3} J/m^2, and ~30.1×10^{-3} J/m^2, respectively. The surface free energies of three substrates are similar. Moreover, the surface free energy of the BPLC mixture is ~30.4×10^{-3} J/m^2 (the red dotted line in Fig. 1(a)) closed to the surface free energies of three substrates. We also measured the contact angles of the mixture on substrates with different surface treatments. In order to figure out the adhesion energy between the mixture and distinct surfaces, we first used a CCD camera (JAI CV-M30) to capture the images of the droplet of the mixture on the surfaces, and then utilized a contact angle measuring system (FTA 1000 Analyzer System) to obtain the contact angles. Figure 1(b) shows contact angle of the mixture at different surface. The contact angles for the PA, ITO, and VA cells were 3.5°, 9.7°, and 18.4°, respectively. The mixture exhibits the largest contact angle on the surface of the VA cell, while the smallest contact angle on the surface of the PA cell. The results in Fig. 1(b) also follows so-called Friedel-Creagh-kmetz rule [25]. To further calculate adhesion energy between the mixture and a substrate, we can use the Young's Equation (Eq. (1)) and Dupre's Equation (Eq. (2)) [24,26]:

#258217 Received 25 Jan 2016; revised 26 Feb 2016; accepted 1 Mar 2016; published 3 Mar 2016

$$\gamma_{sv} = \gamma_{sl} + \gamma_{lv} \times \cos\theta \quad (1)$$

$$\gamma_{sl} = \gamma_{sv} + \gamma_{lv} - \gamma_{adhesion} \quad (2)$$

where γ stands for surface free energy, and lower case s, v and l represent substrate, vapor and liquid. $\gamma_{adhesion}$ represent adhesion energy between the mixture and a substrate. θ represents contact angle. The adhesion energies of the PA, ITO, and VA cells were ~60. 7 × 10^{-3} J/m^2, ~60.4 × 10^{-3} J/m^2, and ~59.3 × 10^{-3} J/m^2. After considering the error of contact angle measurement (i.e. $\pm 2.5^0$), the BPLCs mixture has different adhesion energies among those substrates, which in turn, from large to small, were PA cell, ITO cell, and VA cell. The experimental data are also summarized in Table 1. As a result, three cells we prepared indeed provided different boundary conditions for crystal growth of PS-BPLCs.

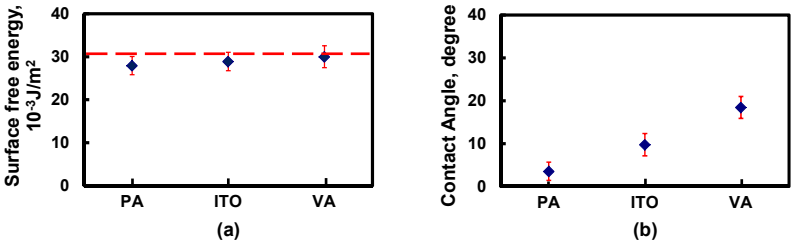

Fig. 1. (a) Measured surface free energy of different substrates. (b) Contact angles of BPLC droplet on different substrates. The red dashed line in (a) indicates the surface free energy of BPLCs in air (30.4x10^{-3}J/m^2)

Table 1. A summary of measured surface free energy, contact angle and calculated the adhesion energy for different cells.

	Surface free energy (10^{-3} J/m^2)	Contact Angle (degree)	Adhesion energy (10^{-3}J/m^2)
PA	28.9	3.5	60.7
ITO	27.9	9.7	60.4
VA	30.1	18.4	59.3

To investigate crystal growth of BPLCs mixture, we first heated the samples (i.e. mixtures in three cells) until the mixture at each cell was at the isotropic state, and then we observed the morphology during the cooling process at a cooling rate of 0.5 °C/min through a reflective polarized optical microscope (POM, Leica DM-2500D). The recorded images for the samples are shown in Figs. 2(a) to 2(i). For the ITO cell, blue phase appeared at 28.9 °C with formation of punctate crystal domains (Fig. 2(a)). When the temperature decreases from 28.9 °C to 26.7 °C, the morphology of the sample exhibits Bragg's reflection with red, green, and blue crystal domains which indicates crystal orientations of [200], [211], and [220], respectively. The crystal orientations could be measured and estimated by Kossel diagram [16, 17]. In addition, the domain size of the mixture turns out to be larger with stronger Bragg's reflection as the temperature decreases. In Fig. 2 (d), the averaged domain size was ~12 μm, which is similar to the previous results we presented [16, 17].Thereafter, we repeated the same cooling process to observe morphologies of the BPLC mixture in the PA cell (Figs. 2(e)-2(h)). Instead of the many domains with different colors in Fig. 2(d), the morphologies of BPLC mixture in PA cell shows dark in the beginning in Fig. 2(e) and then the Bragg's reflection of the mixture shifts to blue (Figs. 2(g) and 2(h)) with a decrease of temperature. In Fig. 2(h), the morphology in the PA cell ends up with uniform crystal orientation as well as a few grain boundaries. From Fig. 2(g)-2(h), the appearance of grain boundary seems to

#258217 Received 25 Jan 2016; revised 26 Feb 2016; accepted 1 Mar 2016; published 3 Mar 2016

indicate that crystal dislocations show up during the crystal growth and then the unstable crystal structure break apart to form the grain boundary.

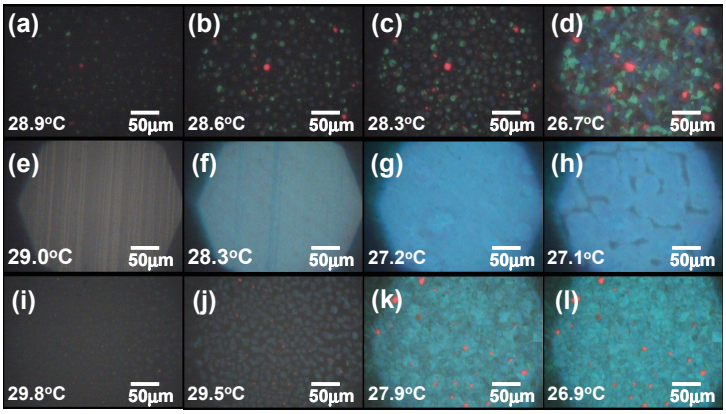

Fig. 2. Morphologies of BPLC mixtures at different temperature under a reflective polarized optical microscope. (a), (b), (c), and (d) are morphologies in the ITO cell. (e), (f), (g), and (h) are morphologies in the PA cell. (i), (j), (k), (l) are morphologies in the VA cell. The cooling rate was 0.5 °C/min.

Figures 2(i) to 2(l) show the morphologies of the VA cell at the cooling process. Similar to those in the ITO cell, the BPLCs first appeared with punctate crystal domains, which have different crystal orientation, as shown in Figs. 2(i) and 2(j). However, the domain sizes of BPLCs were more uniform than those in Fig. 2 (a). When the temperature gradually decreased in Figs. 2(j) to 2(k), the small grains of BPLCs acted like seeds, which enabled BPLCs growing along the sides of grain boundary while maintaining the same crystal orientation. Thus, we could observe more uniform blue crystal domains in VA cell than those in ITO cell. Finally, the whole observation area was full of BPLCs in Fig. 2(l); nevertheless, the grain boundaries indicate that crystal orientation has slightly difference. Comparing the BPLCs growing in cells with different surface treatments, BPLC mixture growing in the PA cell has the highest uniformity of crystal orientation and the BPLC mixture in the VA cell appeared mostly with Bragg's reflection of blue color, while the BPLC mixture in the ITO cell shows random crystal orientations. The grain size of the VA cell is more uniform than the ITO cell, while the BPLCs in the PA cell apparently have less grain boundaries. In addition, the BPLCs in the PA cell quickly appear in the whole region as it takes minutes for those in other two cells to fill the whole observation area. Based on the morphologies in Fig. 2, substrates with different surface treatments indeed have influence on the crystal growth of BPLCs mixtures.

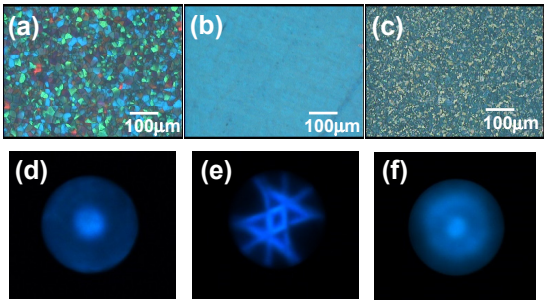

Fig. 3. The observation of PS-BPLCs cell under POM after photo-polymerization (a) ITO cell, (b) PA cell, and (c) VA cell. Kossel diagrams of the PS-BPLCs samples after photo-polymerization at (d) ITO cell, (e) PA cell, and (f) VA cell. λ = 510nm in (d), (e), and (f).

#258217 Received 25 Jan 2016; revised 26 Feb 2016; accepted 1 Mar 2016; published 3 Mar 2016

In order to further investigate the crystal structures of each sample, three cells after cooling process were exposed under UV light for photo-polymerization (i.e. BPLC becomes PS-BPLC) and then observed the Bragg's reflection pattern of the PS-BPLCs. Figure 3 shows the observation under POM as well as Kossel diagrams of the PS-BPLCs in each cell. In Fig. 3(a), the platelet texture of PS-BPLCs in ITO cell shows different wavelength of Bragg's reflection. As for the corresponding Kossel diagram pattern in Fig. 3(d), there are no clear diffraction pattern but only the scattered signals can be observed. That is due to the non-uniform grain size as well as random crystal orientations of PS-BPLCs in Fig. 3(a). As to PA cell in Fig. 3(b), the morphology is uniformly blue and the grain boundary is not clearly observed, slightly different from Fig. 2(h). The hyperbolic lines of the Kossel diagram in Fig. 3(e) indicate that the simple cubic PS-BPLCs are highly uniform with significant large grain size, and the crystal orientation primarily belongs to [220] [4, 16, 17]. As to the VA cell in Fig. 3(c), the observations under POM indicate the crystal orientation are much uniform and the final grain size are smaller than those in ITO cell. In Fig. 3(f), a concentric ring pattern is observed. The diffraction pattern indicates the periodic crystal structure in VA cell with crystal orientation [200] and [300]. Since we assume the lattice constant is invariant and there is no corresponding Kossel diagram like concentric ring, the outer ring seems to be the larger version of the inner ring, which means there exists two similar crystal orientations with different Miller index. We conclude that red crystal domain are likely to represents the crystal orientation with smaller Miller index [200], which corresponds to the obscure outer ring of Kossel diagram. The blue crystal domain represents the similar crystal orientation with large Miller index [300], which corresponds to the clear inner ring.

Based on the experiments, we proposed a possible mechanism of a crystal growth of BPLCs mixture under different conditions of alignment layers, as illustrated in Fig. 4. When the temperature is cooled down from isotropic state gradually (i.e. from T_1, T_2 to T_3), the blue phase and isotropic phase (black region in Fig. 4(a)) of the mixtures coexist. Due to the different wetting properties among the different crystal orientations of the mixtures and the mixtures at the isotropic phase, the ITO cell show many small seeds with different crystal orientations at T_1. Thereafter, the small seeds nucleate to grow up as temperature decreases. The crystal growing rate of different crystal orientations depends on a competition of crystal growth between homogeneous nucleation and heterogeneous nucleation, as depicted in Fig. 4(a). As a result, the morphology of ITO cell after cooling process presents random orientations of BPLC in Fig. 2(d). Figure 3(a) shows the similar morphology because the polymer helps to freeze the BPLC structure through photo-polymerization. We also reported the competition process in our previous results [16, 17].

As to PA cell, the BPLCs mixture has larger adhesion free energy to the PA substrate. That means the mixture tends to spread on the PA substrate, instead of small droplets. Besides, the chemical interaction of the alignment layer results in more uniform crystal orientations. Thus, the spreading drops of the BPLC mixture pin on the substrates and nucleate based on heterogeneous nucleation. As the drop of BPLC mixture nucleated with the cooling process, the BP crystals inside the drop grow as well and might form dislocated boundaries or crystal grains due to a slight mismatch of the crystal orientations, as illustrated in Fig. 4(b). As to the VA cell, the contact angle of BPLC mixture on VA substrate is higher than the ITO cells. Similar to the ITO cell, the mixture starts from a small nucleated seeds on the substrates for heterogeneous nucleation while some seeds locate between substrates for homogeneous nucleation. By influence of chemical interaction of the VA alignment layer, the crystal orientations inside the drops pinned on the substrate tends to align along the same orientation and then grow up for the nucleation during the cooling process. When the adjacent drops touch to each other during nucleation, it results in grain boundaries due to the mismatches of crystal orientations in two drops. This is why we observed the morphology in Fig. 2(l) with many small domains but a uniform color. Some red domains in Fig. 2(l) indicate the homogeneous nucleation. Similar pinning effect of alignment layers to polymer dispersed

#258217 Received 25 Jan 2016; revised 26 Feb 2016; accepted 1 Mar 2016; published 3 Mar 2016

liquid crystals has been reported [27]. When monomer reacts to be polymer, the strong anchoring energy between polymer networks and BPLCs might alter the direction of LC molecule. As we observed PS-BPLCs sample under POM with rotation of the sample in Fig. 3(c), the light intensity of white area does not change much, which means changes of orientation in Fig. 2(l) because of photo-polymerization.

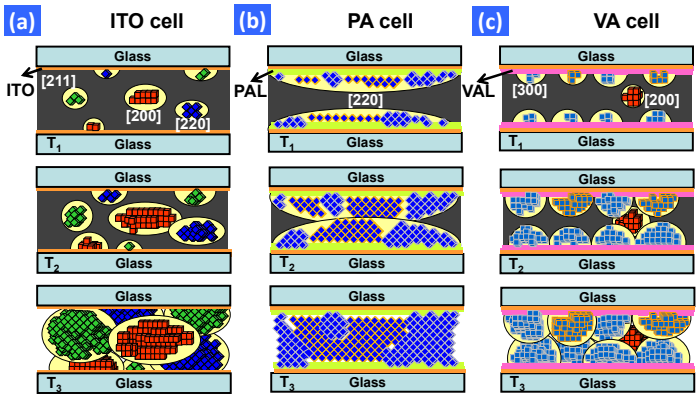

Fig. 4. Possible mechanisms of crystal growth of BPLCs with different surface treatment. (a) ITO cell, (b) PA cell, and (c) VA cell. The orange line represents ITO electrode. The light green line represents the parallel alignment layer (PAL). The pink line represents the vertical alignment layer (VAL). T_1, T_2, and T_3 represent different temperature and $T_1 > T_2 > T_3$.

We also measured the response time and Kerr constant of the PS-BPLCs in all three cells. The measured response times (the sum of the rise time and the fall time) for ITO, PA, and VA samples were 3.04ms, 3.02ms and 2.64ms, respectively. The extended Kerr constants of these three samples were measured around 1.5×10^{-9} m/V^2 [28]. From the measurement results, both of switching times and Kerr constants of the PS-BPLCs remain similar even though the surface treatments were different. The electro-optical properties of the PS-BPLCs are also influenced by the final morphologies. We measured the transmittance of these three cells between two crossed polarizers as a voltage was ramped up and down at λ = 633nm for hysteresis effect. The cells are placed 45 degree with respect to the incident light. The results are shown in Fig. 5. The hysteresis is defined as a difference of applied electric fields when the transmittance is half of saturation transmittance (or highest transmittance) in Fig. 5. The hysteresis values of PA, VA, and ITO cells are 3.54, 4.55, and 4.41 V_{rms}/ μm, respectively. PA cell has slightly low hysteresis while VA cell has slightly high hysteresis. The hysteresis of PA cell exist, this might due to the existence of dislocation, as we can clearly see three groups of hyperbolic lines in the Kossel diagram in Fig. 2(e). By thermal recycling method, ramping the temperature of the crystal growth up and down, the dislocations could be removed and then achieve hysteresis-free [16]. As for VA cell, the morphology of PS-BPLCs is similar to the results of the electrical treatment [17]. The pros of the alignment layers in PS-BPLCs are able to manipulate the morphologies of PS-BPLCs via controlled nucleation process while keeping the similar Kerr constant, and response time. The disadvantage could be the voltage shielding effect from alignment, especially the dielectric anisotropy of the LC host is large [29]. As to the hysteresis, a vertical field switching method can be used to remove hysteresis [30].

#258217 Received 25 Jan 2016; revised 26 Feb 2016; accepted 1 Mar 2016; published 3 Mar 2016

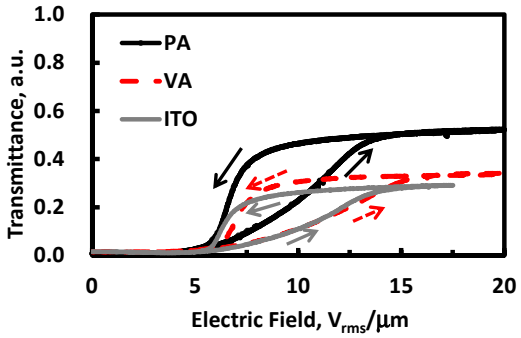

Fig. 5. Transmittance as s function of applied electric field as voltage was ramped up and down. Black line stands, red dotted line, and gray line stand for PS-BPLCs in PA cell, VA cell and ITO cell, respectively.

3. Conclusion

The purpose of this study is to understand how alignment layer affects crystal orientation of PS-BPLCs. Based on the experiments the crystal growth of BPLCs can be affected by means of surface. A possible mechanism was also proposed. When the surface does not have the alignment ability, there exists keen competition between homogeneous nucleation and heterogeneous nucleation, and the BPLC mixture appears with random crystal orientations. With alignment layer, the chemical interaction can help align the LC molecules and a heterogeneous nucleation would dominate during the crystal growth process. Therefore, the morphologies of the BPLCs can be passively manipulated via surfaces with distinct physical properties. The impact of this study is to provide a general understanding how to manipulate the crystal growth of PSBP-LCs and it could help researchers to design better PSBP-LC based devices which requires different morphologies.

Acknowledgments

The authors would like to thank Prof. Ru-Pin Pan (National Chiao Tung University) for the Kossel Diagrams and Prof. Wen-Feng Hsieh (National Chiao Tung University) for discussions. This research was supported by the Department of Natural Sciences and Sustainable Development in the Ministry of Science and Technology (MoST) of Taiwan under contract no. MoST 104-2112-M-009-010-MY3.

#258217 Received 25 Jan 2016; revised 26 Feb 2016; accepted 1 Mar 2016; published 3 Mar 2016